

# Lawrence Berkeley National Laboratory

## LBL Publications

### Title

p+ - p Elastic Scattering at 310 Mev: Recoil-Nucleon Polarization

### Permalink

<https://escholarship.org/uc/item/41v4c9q0>

### Authors

Foote, James H  
Chamberlain, Owen  
Rogers, Ernest H  
et al.

### Publication Date

1960-11-01

### Copyright Information

This work is made available under the terms of a Creative Commons Attribution License, available at <https://creativecommons.org/licenses/by/4.0/>

UNIVERSITY OF  
CALIFORNIA

*Ernest O. Lawrence*

*Radiation  
Laboratory*

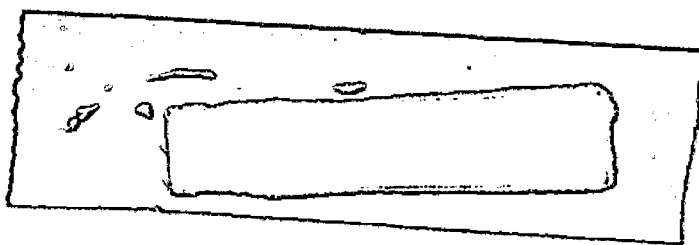
TWO-WEEK LOAN COPY

*This is a Library Circulating Copy  
which may be borrowed for two weeks.  
For a personal retention copy, call  
Tech. Info. Division, Ext. 5545*

BERKELEY, CALIFORNIA

## **DISCLAIMER**

This document was prepared as an account of work sponsored by the United States Government. While this document is believed to contain correct information, neither the United States Government nor any agency thereof, nor the Regents of the University of California, nor any of their employees, makes any warranty, express or implied, or assumes any legal responsibility for the accuracy, completeness, or usefulness of any information, apparatus, product, or process disclosed, or represents that its use would not infringe privately owned rights. Reference herein to any specific commercial product, process, or service by its trade name, trademark, manufacturer, or otherwise, does not necessarily constitute or imply its endorsement, recommendation, or favoring by the United States Government or any agency thereof, or the Regents of the University of California. The views and opinions of authors expressed herein do not necessarily state or reflect those of the United States Government or any agency thereof or the Regents of the University of California.



UCRL-9488  
Limited Distribution

UNIVERSITY OF CALIFORNIA

Lawrence Radiation Laboratory  
Berkeley, California

Contract No. W-7405-eng-48

$\pi^+$ -p ELASTIC SCATTERING AT 310 Mev:  
RECOIL-NUCLEON POLARIZATION

James H. Foote, Owen Chamberlain, Ernest H. Rogers,  
Herbert M. Steiner, Clyde E. Wiegand, and Thomas Ypsilantis

November 16, 1960

$\pi^+$ -p ELASTIC SCATTERING AT 310 Mev:  
RECOIL-NUCLEON POLARIZATION

James H. Foote, Owen Chamberlain, Ernest H. Rogers,  
Herbert M. Steiner, Clyde E. Wiegand, and Thomas Ypsilantis

Lawrence Radiation Laboratory  
University of California  
Berkeley, California

November 16, 1960

## ABSTRACT

The recoil-proton polarization in  $\pi^+$ -p elastic scattering at 310-Mev incident-pion laboratory kinetic energy has been experimentally measured at four scattering angles with scintillation counters. Polarization values obtained, related rms experimental errors, and mean center-of-mass recoil angles are:  $+0.044 \pm 0.062$  at 114.2 deg,  $-0.164 \pm 0.057$  at 124.5 deg,  $-0.155 \pm 0.044$  at 133.8 deg, and  $-0.162 \pm 0.037$  at 145.2 deg. The sign of the polarization is defined to be positive when a preponderance of the recoil protons had their spin vectors pointing in the direction of  $\vec{p}_i \times \vec{p}_f$ , where this quantity is the cross product of the initial and final momentum vectors of the conjugate pions. A beam of  $1 \times 10^6$  pions per sec incident upon a  $1.0\text{-g/cm}^2$ -thick liquid-hydrogen target produced the recoil protons, which were then scattered by a carbon target at a mean energy varying with recoil angle from 113 to 141 Mev. The polarization of the recoil protons was analyzed by measuring the asymmetry produced in the carbon scattering. A proton beam of known polarization was used to determine the analyzing ability (measured asymmetry divided by the polarization of the incident protons) of the system at each recoil angle. Values obtained for the analyzing ability range from 0.41 to 0.57.

$\pi^+$ -p ELASTIC SCATTERING AT 310 Mev:  
RECOIL-NUCLEON POLARIZATION\*

James H. Foote,<sup>†</sup> Owen Chamberlain, Ernest H. Rogers,  
Herbert M. Steiner, Clyde E. Wiegand, and Thomas Ypsilantis

Lawrence Radiation Laboratory  
University of California  
Berkeley, California

November 16, 1960

I. INTRODUCTION

To investigate  $\pi^+$ -p and  $\pi^-$ -p elastic scattering, which are processes of fundamental importance to the understanding of nuclear phenomena, we can measure the differential cross section, the total cross section, and the polarization of the recoil protons as a function of scattering angle.<sup>1</sup> Although pion-proton cross sections have been measured by many experimenters at many energies, the accuracy and completeness of the experimental data can be considerably improved upon. In contrast to the numerous cross-section results, few measurements exist of the recoil-proton polarization in elastic pion-proton scattering. This scarcity of data is due to the difficulty of obtaining pion beams of high energy and, in addition, high intensity. Beams with both of these characteristics are needed so that the polarization of the recoil protons can be satisfactorily analyzed. If the flux of these protons were not adequate or if their energy were too low, we would not be able to determine their polarization with the desired accuracy.

---

\*This work was done under the auspices of the U. S. Atomic Energy Commission.

<sup>†</sup>Now at Lawrence Radiation Laboratory, Livermore, California.

In former analyses of pion-proton scattering data in terms of phase shifts, uncertainties have arisen.<sup>2</sup> Not only have the values and signs of some of the phase shifts in a solution been uncertain, but also several different types of solution have been obtained. Measurements of the recoil-proton polarization can be very useful in removing these uncertainties. Different variations of the polarization with scattering angle are predicted by the various types of phase-shift solutions obtained when only the cross-section data is available. On the basis of polarization measurements, one may therefore be able to decide which type of phase-shift set is the physically valid one. These measurements also improve our knowledge of the individual parameters in a solution because many of the phase shifts are sensitive to the recoil-proton polarization data. The phase shifts related to D waves are especially sensitive to the results of polarization measurements.

There now exists a limited amount of experimental information on the polarization of the recoil protons in  $\pi^{\pm}$ -p elastic scattering. Kunze, Romanowski, Ashkin, and Burger investigated  $\pi^{-}$ -p scattering at 225-Mev incident-pion kinetic energy by using a counter-controlled cloud chamber.<sup>3, 4</sup> In another polarization experiment, Grigor'ev and Mitin examined  $\pi^{+}$ -p scattering at 307 Mev with the aid of photographic emulsions.<sup>5</sup> Vasilevsky and Vishnyakov report preliminary results on the polarization of the recoil protons in  $\pi^{-}$ -p scattering at 300 Mev.<sup>6</sup> They employed approximately 900 Geiger counters to detect the desired events.

There are large experimental errors in all the recoil-proton polarization results just mentioned. Nevertheless, these data have been useful in the analysis of pion-proton scattering. The polarization results have favored certain sets of phase shifts over other sets. (The advent and development of the dispersion relations have also aided in eliminating certain ambiguities.) Information has

been obtained concerning the magnitudes and signs of the  $\pi^+$ -p D-wave phase shifts; however, there are still sizable errors associated with these parameters. Considerable uncertainties also exist in the values of other phase shifts.

Before a precise set of pion-proton phase shifts can be obtained, accurate polarization experiments are needed. In deciding to perform this type of experiment, we have had to consider carefully the problem of obtaining a high-energy, high-intensity pion beam. A beam with the desired characteristics has been produced. It contains positive pions and has a maximum intensity at about 300 Mev. This energy is adequately high so that D waves should be affected by the nuclear interaction, but yet sufficiently low so that only a minimum of inelastic scattering should occur. Inelastic scattering is undesirable because it can complicate the measurements and subsequent analysis.

Our pion beam has now been used to detect the polarization of the recoil protons in  $\pi^+$ -p elastic scattering at 310 Mev. Plastic scintillation counters were used for this purpose, and data were obtained at four different scattering angles.

This report discusses these polarization measurements. We will first present the quantities and equations pertinent to the experiment. Then we describe the pion beam and the method, apparatus, and procedures used to determine the polarization of the recoil protons. The calibration of the apparatus will be included in this discussion. Finally, we will present the results of the polarization measurements and discuss uncertainties in these results.



## II. POLARIZATION FUNDAMENTALS

To order to define polarization and its related quantities, let us employ a right-handed x-y-z Cartesian-coordinate system. The associated spherical angular coordinates  $\theta$  (or  $\Theta$ ) and  $\phi$  (or  $\bar{\phi}$ ) are defined in the customary manner.<sup>7</sup> We consider a beam of protons moving along the z axis in the +z direction, with a scattering target placed at the origin. Let the x and z axes lie in the horizontal plane and allow the +y direction to be up. The component of the polarization vector of the incident proton beam in the direction perpendicular to the horizontal plane can be defined as  $P = (N_U - N_D)/(N_U + N_D)$ , where  $N_U$  and  $N_D$  are the numbers of incident protons per unit beam with their spin vectors pointing up and down, respectively.

If a beam of protons is polarized in the direction perpendicular to the horizontal (x-z) plane and elastically scatters off a target composed of spin-zero nuclei, one can write<sup>8</sup>

$$\bar{e} = \bar{P}_1 \bar{P}_2 . \quad (1)$$

Here  $\bar{P}_1$  is the polarization in the y direction of the incident proton beam,  $\bar{P}_2$  is the polarization that would be generated in the scattering (denoted by the subscript 2) if the incident beam were unpolarized, and  $\bar{e}$ , the asymmetry produced in the scattering, is defined as

$$\bar{e} = \frac{N(\phi_2 = 0^\circ) - N(\phi_2 = 180^\circ)}{N(\phi_2 = 0^\circ) + N(\phi_2 = 180^\circ)} . \quad (2)$$

The quantities  $N(\phi_2 = 0^\circ)$  and  $N(\phi_2 = 180^\circ)$  are the intensities of elastically scattered protons at the designated  $\phi_2$  angles and at the same value of  $\Theta_2$ .

We now apply these results to our recoil-proton experiment, where the subscript 1 refers to the  $\pi^+ - p$  scattering, which produces the protons with polarization

$\bar{P}_1$  (in the  $y$  direction), and the subscript 2 denotes the scattering that analyzes the recoil-proton polarization by producing an asymmetry. Both scatterings are assumed to take place in the horizontal plane. The bars over  $\bar{e}$ ,  $\bar{P}_1$ , and  $\bar{P}_2$  indicate that we are concerned with average values of these quantities, because our pion beam, counters, and targets all have extended dimensions.

The scattering of a polarized beam in order to determine its polarization is referred to as an "analyzing" scattering. A proton that has been scattered and then detected is designated an "analyzed" proton. The factor  $\bar{P}_2$  in Eq. (1) is called the "analyzing ability" of the arrangement. This is not to be confused with the "analyzing efficiency," which is defined later.

We have discussed only elastic scattering in this section. When protons are incident upon an analyzing target such as carbon, inelastic scattering can also occur. Although some kinds of inelastic processes may produce as large an asymmetry as the elastic scattering, other types do not. Thus the inelastic reactions tend to lower the average measurable asymmetry. One wishes to measure as large an asymmetry as possible, consistent with a satisfactory counting rate, to minimize the influence of errors that affect the asymmetry by a fixed amount. We therefore try to arrange the experimental conditions so as to discriminate against as many of the inelastic processes as possible.

According to Eq. (1), we can ascertain the recoil-proton polarization,  $\bar{P}_1$ , by measuring  $\bar{e}$  and  $\bar{P}_2$ . Our asymmetry measurements will be described in Sections III and IV. The determination of  $\bar{P}_2$  will be discussed in Section V.

### III. BEAM, METHOD, AND APPARATUS

#### A. Positive-Pion Beam

The external proton beam of the 184-in. synchrocyclotron at Berkeley produced the desired positive pions. At the point where it entered the experimental area (Physics Cave), the proton beam was about 2.5 in. wide and 1.5 in. high. It had an energy of approximately 743 Mev, a root-mean-square (rms) energy spread of about  $\pm 8$  Mev, and a maximum intensity of  $(2 \pm 1) \times 10^{11}$  particles per sec.

A polyethylene ( $\text{CH}_2$ ) target was placed in the external proton beam near the point at which the beam entered the cave (see Fig. 1). This material was selected principally on the basis of its free-proton constituent ( $\text{H}_2$ ), which can enter into the  $p + p \rightarrow \pi^+ + d$  process. We were able to obtain an optimum number of 310-Mev pions by taking maximum advantage of this reaction. The thickness of the  $\text{CH}_2$  was experimentally determined to give the maximum number of positive pions leaving the target in the forward direction with the desired energy. The optimum target thickness was about 19 in.

After leaving the polyethylene target, the positive pions with the requisite energy were momentum-analyzed and focused by a series of two bending and three quadrupole focusing magnets (Fig. 1). The first focus of the system was within the center quadrupole magnet. This magnet acted on the off-axis particles to increase the number reaching the final focus, which was at the liquid-hydrogen target shown in Fig. 1. In order to obtain the desired physical arrangement, the second bending magnet was built into the concrete shielding surrounding the cave. A 2-in.-thick piece of carbon absorber was placed directly after the central focusing magnet in order to remove low-energy particles with the selected momentum, such as protons, from the beam.

The symmetry of the magnet arrangement enabled the second half of the system to approximately cancel the momentum dispersion created by the first half. Thus a distinct final focus was obtained in which there was little correlation between momentum and position across the beam. The  $\pi^+$  beam was observed to be nearly symmetrical at the final focus in both the horizontal and vertical directions. Its full width and height at half maximum intensity were about 3 in. and 2 in., respectively.

At the center of the liquid-hydrogen target, the mean energy of the pions was 310 Mev (momentum of 427 Mev/c), and the maximum intensity was about  $2 \times 10^6$   $\pi^+$  mesons per sec.<sup>9</sup> The rms uncertainty in the mean energy of the beam was approximately  $\pm 3$  Mev, and the rms energy spread in the beam was  $\pm 10$  Mev, corresponding to a momentum spread of  $\pm 2.5\%$ . The energy of the pions was measured by determining their range in copper, and also by the suspended-wire technique.

#### B. Method

A small fraction of the incident positive pions elastically scattered on protons in the liquid-hydrogen target. In terms of the nomenclature in Fig. 2, counters A and B selected the recoil protons that left the target at angles approximating  $\Theta_1$ . Counter C was placed at the appropriate angle ( $\Theta_C$ ) to count the elastically scattered pions that had knocked protons in the AB direction. This counter placed a severe restriction on the type of scattering event that could be detected by the system. In general, events other than elastic  $\pi^+$ -p scattering could not produce a count in C as well as a particle through A and B. Counter C was surrounded by 2.4-g/cm<sup>2</sup>-thick iron, which helped guard against low-energy charged particles.

A portion of the recoil protons, after passing through counters A and B, were scattered by the carbon analyzing target placed immediately following B. We chose carbon as the material for this target because of its ability to analyze the polarization of protons in the energy region of our recoil protons (110 to 140 Mev). <sup>10</sup> Counter B played a dual role in that it also served as part of the analyzing target. Carbon being one of its principal constituents, counter B produced about the same asymmetry as did the actual carbon target.

The two counter telescopes shown in Fig. 2 detected protons that were scattered by the analyzing target. Copper absorber was placed between the counters in each telescope to help prevent unwanted particles from counting in  $D_O$  or  $D_E$ . The counter telescopes were interchangeable in position. In this way, each independently measured the asymmetry produced by the analyzing scattering. The second telescope increased our counting rate and served as a check on the first set of counters. The size of  $D_O$  and  $D_E$  was chosen so that these counters accepted almost all the scattered protons detected by counters III and IV.

Because of the low counting rates expected, counters with large areas were used. We had to reach a compromise, however, between counting rate and angular resolution. The sizes of the counters in the analyzing telescopes were limited because of the undesirability of excessively lowering the average measurable asymmetry. Immoderately large counters would extend over an excessively great range of the analyzing angles  $\theta_2$  and  $\phi_2$ . Only over certain regions of values of these angles are both the asymmetry and counting rate satisfactory. As  $\phi_2$  approaches 90 and 270 deg, the asymmetry disappears

[because, at  $\phi_2$  angles other than 0 and 180 deg, a  $\cos(\phi_2)$  factor enters into Eq. (1)<sup>11</sup>]. If  $\theta_2$  is too small, the asymmetry due to nuclear scattering is considerably lower than the maximum obtainable value,<sup>10</sup> and also the unpolarized Coulomb scattering can enter. At large values of  $\theta_2$  the intensity of the scattered protons decreases greatly,<sup>10</sup> and the effects of inelastic scattering increase.

In order to limit the spread of recoil angles accepted by the system and to aid the  $\theta_2$  angular resolution, counters A and B were made smaller than those employed in the analyzing telescopes. The estimated rms spread in the  $\theta_1$  values of the accepted recoil protons was  $\pm 2.4$  deg [corresponding to  $\pm 4.8$  deg in the center-of-mass (c. m.) scattering angle]. This number did not vary appreciably over the range of recoil angles investigated. Principal sources of the spread in  $\theta_1$  were (estimated rms values are given):

- |  |                |
|--|----------------|
| (a) counter size                                 | $\pm 0.8$ deg  |
| (b) pion beam convergence                        | $\pm 1.8$ deg  |
| (c) beam width and liquid-hydrogen-target length | $\pm 1.3$ deg. |

The rms sum of these numbers is the value of 2.4 deg just presented.

### C. Counters, Electronics, and Scattering Apparatus

Each counter was composed of polystyrene plastic scintillator and was viewed by one RCA-6810 photomultiplier tube. A solid lucite light pipe connected each photomultiplier to its corresponding scintillator. The dimensions of the scintillating regions of the counters (all rectangular in area) are given in Table I.

Our electronics arrangement employed fast coincidence circuits of the Wenzel type<sup>12</sup> to detect the scattering events of interest. Output pulses from each of the counters were delayed and amplified when necessary, and fed into

the coincidence circuits. A coincidence between pulses from counters A, B, and C detected  $\pi^+$ -p scattering events at the liquid-hydrogen target. The output pulse from the ABC coincidence was amplified, split, and fed into two additional coincidence circuits. One of these circuits accepted pulses from counters III and  $D_O$ ; the other received pulses from IV and  $D_E$ . In this manner, coincidences were formed of the types ABC III  $D_O$  and ABC IV  $D_E$ . The output pulses representing the five-fold coincidences, and also an ABC output pulse, were amplified, passed through amplitude discriminators, and finally were fed into scaling units.

The liquid-hydrogen target, with slight modification, was that described by Chamberlain and Garrison.<sup>13</sup> The amount of liquid hydrogen in the scattering plane was approximately  $1.0 \text{ g/cm}^2$ . In order to determine the portion of our final counting rate not due to the liquid hydrogen, a second target assembly was also employed. This "blank" was similar in construction to the liquid-hydrogen target assembly but contained no hydrogen. When desired, the actual target was moved out of position and the evacuated blank placed on the beam line.

Our counters, targets, and principal supporting frameworks are shown in Fig. 3. (Counter C is not included in the drawing.) Distances between counters and targets are given in Table II. As indicated in Fig. 3, the analyzing angles were measured by means of a plumb bob attached to each counter telescope.

#### IV. EXPERIMENTAL PROCEDURES

##### A. General Procedures

The appropriate voltages at which to set our counters and the proper amounts by which to delay the pulses from the counters were determined by observing coincidence counting rates as a function of these parameters. In ascertaining the voltage and delay settings, we examined particles that were of the same type and energy as those to be investigated in the asymmetry measurements. We therefore adjusted the system to count the desired particles and to discriminate against unwanted particles. After selecting the final voltages, time delays, and amplifier settings, a simultaneous change of  $\pm 50$  v in all the counter voltages did not significantly alter the counting rates. On many occasions during the data-accumulating period, this test was performed as a check on the stability of the electronics.

Background particles posed a considerable problem at the beginning of the experiment. Much of the background was produced by the external proton beam of the cyclotron stopping in the rear wall of the cave. In anticipation of difficulty, we solidly embedded the second bending magnet in the cave wall, placed concrete roof blocks on the cave, and put concrete above, below, and on both sides of the last focusing magnet. These precautions were not sufficient. We were able to further reduce the accidental counting rate by using the fast electronics already described and by employing as long a cyclotron beam spill as possible. We finally were forced to lower the intensity of the external proton beam, and therefore the pion beam, by a factor of two (the resulting  $\pi^+$  intensity was  $1 \times 10^6$  per sec).

To determine our accidental counting rate, we delayed the ABC coincidence output pulse by  $5.2 \times 10^{-8}$  sec before it entered into a coincidence of the type ABC III D<sub>O</sub> or ABC IV D<sub>E</sub>. This amount of delay represented



the time difference between two radio-frequency fine-structure pulses of the cyclotron. We investigated singles rates and various coincidence rates, and concluded that our principal source of accidentals was a valid ABC event forming a coincidence with a second particle that passed through one of the sets of analyzing counters. The accidentals were reduced by piling lead bricks near counter B, as shown in Fig. 2. This lead shielding extended approximately 1 ft above and below the beam line. It limited the number of particles that could pass through the analyzing counters without also passing through A and B. At our smaller recoil angles, the lead wall nearer the pion beam was extended until it almost completely shielded the analyzing counters from the beam. We placed additional lead shielding, at all recoil angles, just before the liquid-hydrogen target. This shielding was put on the same side of the pion beam as the scattering arm and eliminated many particles that scattered off or near the last focusing magnet.

The region of laboratory recoil angles investigated was 17 to 32 deg. The recoil angle  $\Theta_1$  could not be made excessively small, or the set of analyzing counters nearer the pion beam would extend into the beam. We were limited at the other extreme by the desirability of obtaining a relatively high average energy at the analyzing scattering. As explained earlier, it was advantageous to measure as large an asymmetry as feasible. For a given incident proton polarization, the asymmetry that can be produced by carbon decreases rapidly below 135 Mev.<sup>10</sup> We therefore did not want the average scattering energy at the carbon target to fall much below this value. Our recoil angles were thus restricted to the forward direction in the laboratory system, corresponding to large angles of scattering in the c. m. system. We used thinner carbon targets at the larger recoil angles to compensate at least partially for the decrease in energy of the recoil protons.

The range of  $\Theta_2$  values (analyzing-telescope angles) used in the asymmetry measurements was 15.5 to 17.0 deg. In deciding upon these settings, we compromised between various factors. These factors, which were discussed in Section III-B, include inelastic scattering, counting rate, and magnitude of the asymmetry.

On at least one occasion during the experiment, we observed the ABC counting rate with no liquid hydrogen in the target. We compared the counting rate when the evacuated target assembly was on the beam line with the corresponding rate when the blank was in position. The agreement was found to be satisfactory for the polarization measurements, and therefore the blank was considered a reliable facsimile of the actual target assembly.

On another occasion during the experiment, we removed the carbon analyzer and left only counter B to scatter the recoil protons. The rate of analyzed protons decreased by approximately the predicted amount, thereby increasing our confidence in the experimental method.

A few more comments about our general experimental procedures are in order before we discuss specific procedures at each recoil angle. An argon-filled ionization chamber was placed in the pion beam before the liquid-hydrogen target in order to monitor the beam intensity. Our counting rates were normalized to a standard amount of beam through the ionization chamber. Because the polarization measurements did not require a knowledge of the absolute intensity of  $\pi^+$  mesons striking the target, no corrections were made for beam contamination. For each of four values of  $\Theta_1$ , we analyzed, under the same conditions, the polarization of the protons recoiling to both the left and right sides of the pion beam (in the horizontal plane). The two resulting asymmetries at each  $\Theta_1$  were then compared. These two asymmetries should have the same magnitude but opposite sign. The agreement generally obtained served as a check on the experimental method.

### B. Procedures at Each Recoil Angle

We began the data collecting at each recoil angle by determining the range of the recoil protons. During these measurements, the angle  $\Theta_2$  of the selected analyzing telescope was set near 0 deg and the carbon target to be used in the asymmetry determination was in its position immediately after counter B. One of our range curves is shown in Fig. 4. At the recoil angles initially investigated, range curves for both sets of analyzing counters were obtained. We found satisfactory agreement between the two telescopes, and subsequently measured only one range curve at each recoil angle. Equal ranges were also observed for protons recoiling to the left and right sides of the pion beam at a given value of  $\Theta_1$ . The mean energies of the protons, as determined from the range curves, agreed well with the predictions of kinematics. An examination of the tails on the range curves indicated that about 97% of the detected particles were the desired recoil protons.

The running point, indicated by an arrow in Fig. 4, refers to the amount of copper absorber that was placed between the counters in each analyzing telescope during the asymmetry measurements. The copper partially guarded against particles associated with inelastic-scattering processes in the liquid-hydrogen and carbon targets and stopped a portion of the stray background particles. At the same time, the absorber permitted the detection of the recoil protons that were elastically scattered at the analyzing target.

Following the range-curve measurements, we obtained the profile of the recoil-proton beam defined by the ABC coincidences. Each analyzing telescope was individually moved through this beam and counting rates determined at various angular settings. The profile and subsequent asymmetry measurements

were made under as identical conditions as possible. In particular, both series of measurements used the same analyzing target and the same amount of copper before  $D_O$  and  $D_E$ . A beam profile is shown in Fig. 5. The center line was determined from the experimental data and represents the center, horizontally, of the beam of detected recoil protons.

After obtaining a range curve and two beam profiles at a selected recoil angle, we measured the asymmetry of the recoil protons that scattered off the carbon target. No variation of asymmetry with beam intensity was found as long as the pion intensity did not exceed  $1 \times 10^6$  particles per sec. The analyzing telescopes were regularly interchanged in order to allow each set of counters independently to measure the asymmetry. By alternating the telescopes frequently, we reduced the adverse effect of slow time variations in the equipment on the asymmetry measurements. The left and right analyzing angles for each telescope were set with respect to the center line of the profile obtained with that telescope. In this way, we minimized the influence of differences in the two counter arrangements on the measured asymmetries. Systematic errors in the asymmetries were lessened by accurately determining with each telescope the center line of the recoil-proton beam, and by precisely setting the analyzing angles. The profiles were checked frequently during the asymmetry measurements by repeating two observations on each side of the center line.

With the telescopes positioned at the appropriate analyzing angles, a series of counting rates was determined. The ABC III  $D_O$  and ABC IV  $D_E$  rates were obtained for the following experimental arrangements:

- (a) liquid-hydrogen target centered on the pion beam, and normal time delays
- (b) liquid-hydrogen target centered on the pion beam, and the ABC pulse delayed by  $5.2 \times 10^{-8}$  sec (accidental rate)
- (c) blank centered on the pion beam, and normal time delays.

The accidental rate with the blank centered on the beam was found to be negligible and was therefore not measured regularly. We obtained the rate of analyzed recoil protons by subtracting the rates in (b) and (c) from that in (a), and by combining the statistical counting errors in the appropriate manner. The difference between left and right analyzed-proton rates, divided by the sum of these rates, then gave the asymmetry,  $\bar{e}$ .

The types of particles that we wished to detect in measurement (c) may have passed through the liquid hydrogen during the (a) measurement. If this were the case, rate (c) should have been determined with additional copper absorber before  $D_O$  and  $D_E$  in order to compensate for the ionization energy loss in the absent liquid hydrogen. The rate in (c) was observed with and without the added absorber, and no difference was detected. Therefore we generally neglected this copper correction.

Significant experimental quantities are listed in Table III. Included are pertinent angles and energies, analyzing-target thicknesses, five-fold coincidence counting rates, and analyzing efficiencies. Our final five-fold counting rates were limited by the number of ABC coincidences. The ABC rate, in turn, was restricted by counter B and to a smaller extent by counters A and C. The accidental and blank corrections each averaged about 5% of the corresponding corrected analyzed-proton rate. The rms energy spread of the recoil protons, as determined from the range curves, did not vary greatly with angle and was typically about  $\pm 10$  Mev.

## V. CALIBRATION AND INITIAL POLARIZATION MEASUREMENTS

### A. Calibration

As explained in Section II, the formula  $\bar{e} = \bar{P}_1 \bar{P}_2$  is applicable to the experiment under discussion here. In order to obtain  $\bar{P}_1$  at various recoil angles, we measured  $\bar{e}$  and  $\bar{P}_2$ . We have described how  $\bar{e}$  was determined. The calibration portion of the experiment, in which we measured the analyzing ability,  $\bar{P}_2$ , will now be discussed.

The analyzing ability of an experimental arrangement depends on characteristics of the incident proton beam, analyzing target, and detecting counters, but is independent of the polarization of the incident protons. Examples of quantities affecting  $\bar{P}_2$  are the energy of the polarized protons at the analyzing target, the type and thickness of material composing the target, the angles subtended by the counters measuring the asymmetry, and the amount of copper absorber in the analyzing telescopes. If all components and characteristics of the system are identical for two different asymmetry measurements, then the analyzing abilities are the same.

In order to determine the analyzing ability of our system for each measured recoil-proton asymmetry, we employed a proton beam of known polarization. The polarized protons passed through counters A and B, scattered on the analyzing target, and were detected by the same analyzing telescopes as those employed in the recoil-proton measurements. Corresponding to the recoil-proton investigations, the analyzing scattering took place in the horizontal plane and the incident protons were polarized in a direction perpendicular to this plane. Equation (1) can be rewritten for the calibration portion of the experiment as  $\bar{e}^{(C)} = \bar{P}_1^{(C)} \bar{P}_2^{(C)}$ . By knowing

$\bar{P}_1^{(C)}$  and by measuring  $\bar{e}^{(C)}$ , we could experimentally determine  $\bar{P}_2^{(C)}$ . If the conditions under which we obtained  $\bar{P}_2^{(C)}$  were the same as those in the measurement of a recoil-proton asymmetry, then  $\bar{P}_2^{(C)}$  is equal to the recoil-proton analyzing ability that we wished to ascertain. Because the characteristics of the analyzing scattering were different for each recoil angle (see Table III), four separate analyzing abilities had to be determined. This method of obtaining the values of  $\bar{P}_2$  took into account the small portion of the analyzed recoil protons that had been inelastically scattered at the carbon target.

We produced the proton beam of known polarization by passing unpolarized protons through the magnet system shown in Fig. 1 and scattering them off a carbon target placed at the final focus. The protons were obtained by degrading the external proton beam of the cyclotron as it entered the Physics Cave. With the 2-in. -thick carbon absorber removed from its position after the central focusing magnet, the degrader thickness and the magnet currents were adjusted to give an unpolarized proton beam of the desired energy. The proton-beam size at the final focus of the magnet system was nearly the same as that of the  $\pi^+$ -meson beam. The liquid-hydrogen target used in the recoil-proton measurements was replaced by a carbon target measuring 0.25-in. thick by 6-in. wide and 8-in. high, which was centered on the beam line. A range curve of the unpolarized proton beam showed the fraction of mesons in the beam to be negligible and the mean energy of scattering in the carbon to be 173 Mev.

The scattering arm was placed so that counters A and B accepted a mean scattering angle of about 13.8 deg (left). By using data from Dickson and Salter,<sup>10</sup> Tyrén et al. and Alphonse et al.,<sup>14</sup> and Hafner,<sup>15</sup> we calculated the mean polarization of the scattered protons detected by counters A and B to be  $0.71 \pm 0.05$  (in the direction perpendicular to the plane of scattering). We included

the effects of inelastic scattering in this calculation. Although a higher elastic-scattering polarization could have been obtained at a larger angle, the relative importance of the less-desirable inelastic scattering would have been increased. The rms error of  $\pm 0.05$  in the polarization is based on uncertainties in the elastic and inelastic experimental data employed in the calculation of the polarization, and uncertainties in the distribution and values of the scattering angles accepted by counters A and B.

Using the polarized-proton beam defined by counters A and B, we reproduced the different sets of recoil-proton analyzing conditions as closely as possible and measured the four resulting asymmetries. In order to obtain the required mean scattering energies at the analyzing targets, sufficient amounts of degrader were placed just before counter A. The thickness of degrader was different for each of the four measurements. Range curves showed that we had attained the same mean scattering energies as in the recoil-proton observations to within about 2 Mev. The rms energy spread in the polarized-proton beam was  $\pm 8$  Mev, slightly less than the  $\pm 10$ -Mev energy spread of the recoil protons. For each of the four calibration measurements, a beam profile was obtained with each analyzing telescope and the appropriate analyzing angles were set with respect to the observed center lines. The positions of these profile center lines were not the same as in the recoil-proton measurements owing to the differences in the angular distributions of the protons from  $p-C$  and  $\pi^+-p$  scattering.

Data were obtained in the calibration measurements by observing the AB III  $D_O$  and AB IV  $D_E$  coincidence rates. Counter C could not be employed in the calibration procedures because the conjugate particles (carbon nuclei) received too little energy to be counted. We determined the "blank" rate by removing the 0.25-in. -thick carbon target from its position in the unpolarized-proton



beam. The calibration counting rates, after correcting for accidental and blank counts, were approximately ten times the rates in the recoil-proton measurements. Our accidental coincidences averaged about 5% of the corresponding corrected analyzed-proton rate, and the target-out (blank) coincidences averaged about 14%. Much higher counting rates could have been obtained by raising the intensity of the external proton beam of the cyclotron. We restricted our net counting rate in order to limit the accidental and blank coincidences to reasonable levels. The effect of background particles was reduced by stacking lead bricks at the same positions as in the recoil-proton measurements.

### B. Initial Polarization Measurements

Our data on the polarization of the recoil protons were obtained during two different running periods at the cyclotron. In general, the procedures and the apparatus were the same in both runs. Where differences existed we have referred to the Run-2 arrangement, as a preponderance of our data was acquired during the second period. Owing principally to the larger-area telescope counters employed in the first run, the analyzing abilities measured then were smaller than those later obtained. The polarized proton beam used in the calibration portion of Run 1 had a polarization of  $0.58 \pm 0.09$ . Only one analyzing telescope was employed in the initial polarization measurements.

During the recoil-proton measurements in the first run, we photographed the pulses from the counters as a check on the performance of the electronics. Signals from the counters were displayed on a four-beam oscilloscope. Whenever the electronics detected a possible five-fold coincidence, the oscilloscope was triggered and the pulses appearing on the four sweeps were recorded on 35-mm film. The film was later projected on a viewer. We measured and plotted the heights and relative positions of the pulses from each counter.

The resulting distributions enabled us to select restrictive criteria for the validity of an event. We rejected a set of pulses if the position or height of any individual pulse did not closely conform to the appropriate normal value. The acceptable film events determined an asymmetry at each recoil angle. There was no blank counting rate to be subtracted; blank coincidences were negligible during the early measurements owing to the relatively low intensity of the pion beam. Accidentals that could deceive the electronics were presumably eliminated in the film analysis because of the restrictive criteria. Values of the asymmetries calculated from the film data agreed well with the electronic asymmetries and increased our confidence in the electronic method.

## VI. ERRORS AND RESULTS

### A. Experimental Errors

Principal sources of experimental error in the asymmetry measurements were counting statistics and uncertainty in the center line of the recoil-proton beam. Uncertainty in the position of the center line can arise, for example, from variations in the direction of the  $\pi^+$ -meson beam due to magnet-current fluctuations. Another source of this type of error is in the determination of the beam-profile center line from the observed profile counting rates.

We obtained an estimate of the uncertainty in the position of the recoil-proton-beam center line by examining the variation at each recoil angle of the observed beam-profile center lines. It was assumed that these fluctuations reflected the various sources of error and therefore gave an approximate experimental determination of the composite uncertainty. This investigation yielded an rms error in the profile center line of  $\pm 0.10$  deg for Run 1 and  $\pm 0.06$  deg for Run 2. We calculate that an error of 0.10 deg in the position of the beam center line causes an uncertainty of approximately 0.02 in the measured asymmetry. Thus the estimated error in each asymmetry measurement due to this origin is  $\pm 0.020$  for Run 1 and  $\pm 0.012$  for Run 2. These numbers are based on the recoil-proton observations but also appear approximately valid for the calibration portions of the experiment.

We estimate an rms uncertainty of  $\pm 0.45$  deg in each mean laboratory recoil angle given in Table III. This corresponds to an error of about  $\pm 0.90$  deg in each c. m. scattering angle. Principal sources of this error are uncertainties in: the position and direction of the pion beam at the liquid-hydrogen target, the position of counter B, the position of the liquid-hydrogen target along the beam line, and the correction applied in order to obtain the mean recoil angle from the angle at the geometric center of counter B. In the calibration for Run 2, these sources of error yield an rms uncertainty of  $\pm 0.6$  deg in the mean laboratory scattering angle accepted by counters A and B.

### B. Experimental Results

Tables IV and V present the experimental results of both runs. The satisfactory agreement that was obtained between the two sets of analyzing counters in Run 2 is not shown; only the combined results are presented. When combining two asymmetry or polarization measurements, the individual quantities have been weighted by the inverse of the square of their errors.

The uncertainty in the polarization of each calibration proton beam is not included in the errors given in Table V. Thus there is an additional rms error of  $\pm 15.5\%$  in all Run-1 values of  $\bar{P}_2$  and  $\bar{P}_1$ , and of  $\pm 7\%$  in all Run-2 values. When combining the polarization results of the two runs, we neglected this type of uncertainty. The 15.5% error in Run 1 and 7% error in Run 2 are partially correlated because they are based to a certain extent on the same experimental scattering data. Even if these errors were completely correlated, which is not the situation, the maximum possible effect on any of our final (combined) polarization values would be an additional rms uncertainty of only  $\pm 11\%$ . This is small compared with the final errors given.

Our sign conventions will now be summarized. In Table IV, the sign of the asymmetry is considered positive if more of the recoil protons scattered to the left than to the right at the carbon target. A positive analyzing ability in Table V signifies that a majority of the protons scattered to the left at the analyzing target when a preponderance of the incident protons had their spin vectors pointing up (out of the plane of Fig. 2). The sign of the recoil-proton polarization is positive in Table V when more than half of the protons had their spin vectors pointing in the direction of  $\vec{p}_i \times \vec{p}_f$ , where this quantity is the cross product of the initial- and final-momentum vectors of the conjugate pions. In other words, a positive polarization signifies that a majority of the protons recoiling to the right side of the incident pion beam had their spin vectors pointing up.

The four final polarization values given in Table V have been combined with accurate cross-section data at 310 Mev, and a comprehensive phase-shift analysis performed. These polarization measurements have had a definite influence on the results of the analysis and have enabled us to investigate the  $\pi^+$ -p phase shifts more thoroughly than was previously possible. The phase-shift investigations employing the four polarization values are discussed elsewhere.<sup>16</sup>

#### ACKNOWLEDGMENTS

The support of Professor Emilio Segrè is gratefully acknowledged. Much conscientious assistance during the experimental work was provided by Dr. Janice Button, Dr. Rudolph R. Larsen, Mr. Joseph T. Lach, and Mr. Olav T. Vik. Also greatly appreciated was aid given by Messrs. Leonard B. Auerbach, Robert B. Bacastow, William B. Johnson, and Hugo R. Ruge. The required high-intensity proton beam was reliably furnished by the crews at the 184-in. synchrocyclotron under the supervision of Mr. James T. Vale and Mr. Lloyd B. Houser.

FOOTNOTES

1. Fermi first showed, theoretically, that one can in general expect the recoiling protons to be polarized, this polarization being perpendicular to the plane of the scattering. See E. Fermi, *Phys. Rev.* 91, 947 (1953).
2. For further discussion of the analysis of pion-proton data in terms of phase shifts, refer to J. H. Foote, O. Chamberlain, E. H. Rogers, and H. M. Steiner, University of California Radiation Laboratory Report UCRL-9481, November 16, 1960; submitted to *Phys. Rev.*
3. J. F. Kunze, T. A. Romanowski, J. Ashkin, and A. Burger, *Phys. Rev.* 117, 859 (1960).
4. All energies mentioned in this report are in the laboratory system.
5. E. L. Grigor'ev and N. A. Mitin, *Soviet Physics JETP* 37(10), 295 (1960).
6. See B. Pontecorvo, *Proceedings of 1959 International Conference on Physics of High-Energy Particles, Kiev* (unpublished), p. 38.
7. The angle  $\theta$  (or  $\Theta$ ) is measured with respect to the  $+z$  axis, and  $\phi$  (or  $\bar{\phi}$ ) is measured in the  $x$ - $y$  plane with respect to the  $+x$  axis, the  $+y$  axis lying at  $\phi$  (or  $\bar{\phi}$ ) = 90 deg. In this report, we designate general laboratory scattering angles by  $\theta_i$  and  $\phi_i$ , and laboratory angles at the centers of the scintillation counters by  $\Theta_i$  and  $\bar{\Phi}_i$ , where  $i$  is an identifying subscript (1, 2, or C).
8. For example, see Eq. (7) of O. Chamberlain, E. Segrè, R. D. Tripp, C. Wiegand, and T. Ypsilantis, *Phys. Rev.* 102, 1659 (1956).
9. The beam intensity employed in the polarization measurements is given in Section IV-A.
10. J. M. Dickson and D. C. Salter, *Nuovo cimento* 6, 235 (1957).
11. See Eq. (6) of the work cited in footnote 8.

12. William A. Wenzel, Millimicrosecond Coincidence Circuit for High-Speed Counting, Lawrence Radiation Laboratory Report UCRL-8000, Oct. 1957.
13. O. Chamberlain and J. D. Garrison, Phys. Rev. 103, 1860 (1956).
14. H. Tyrén and Th. A. J. Maris, Nuclear Physics 4, 637 (1957);  
P. Hillman, A. Johansson, and H. Tyren, Nuclear Physics 4, 648 (1957);  
Th. A. J. Maris and H. Tyrén, Nuclear Physics 4, 662 (1957);  
R. Alphonse, A. Johansson, and G. Tibell, Nuclear Physics 4, 672 (1957).
15. E. M. Hafner, Phys. Rev. 111, 297 (1958).
16. Foote, Chamberlain, Rogers, and Steiner, op. cit.

**Table I. Dimensions of the scintillation counters used to measure the polarization of the recoil protons**

Counter	Dimensions of counter (width $\times$ height $\times$ thickness) (in.)
A	$2 \times 6 \times 1/4$
B	$2 \times 8 \times 1/4$
C	$12 \times 12 \times 1$
III, IV	$4 \times 20 \times 3/4$
$D_O$ , $D_E$	$6 \times 22 \times 3/4$

**Table II. Distances between centers of components of the apparatus used to measure the polarization of the recoil protons**

From	To	Distance (in.)
Liquid-hydrogen target	Counter C	16.5 - 19.25 (depending on $\theta_1$ )
Liquid-hydrogen target	Counter A	24
Counter A	Carbon target	24
Carbon target	Counter III or IV	37.5
Counter III or IV	Counter $D_O$ or $D_E$	5.5



Table III. Significant experimental quantities--angles, analyzing-target thicknesses, energies, five-fold coincidence counting rates, and analyzing efficiencies--for the four mean laboratory angles of detected recoil protons.

Experimental quantity	Mean laboratory angle of detected recoil protons <sup>a</sup> (deg)			
	16.6	22.1	26.6	31.6
Laboratory angle of conjugate pions (deg)	131.6	117.2	106.2	94.7
C. m. scattering angle (deg) <sup>b</sup>	145.2	133.8	124.5	114.2
Analyzing-telescope angle, $\Theta_2$ (deg)	15.5	15.5	17.0	17.0
Thickness of carbon analyzing target (in.)	2.0	1.0	0.5	0.5
Mean kinetic energy of recoil protons at center of liquid- hydrogen target (Mev)	178	167	154	139
Mean kinetic energy of con- jugate pions at center of liquid-hydrogen target (Mev)	132	143	156	171
Mean kinetic energy of recoil protons at center of carbon analyzing target (Mev)	141	140	128	113
Approximate average ABC III D <sub>O</sub> or ABC IV D <sub>E</sub> coincidence rate per minute <sup>c</sup>	5	2	1	1
Approximate analyzing efficiency of <u>each</u> telescope <sup>d</sup>	1/300	1/600	1/1100	1/700

<sup>a</sup> Because of the angular variation in the differential cross section, each mean laboratory angle is about 0.3 deg smaller than  $\Theta_1$ , the corresponding angle at the center of counters A and B.

<sup>b</sup> The angle in the c. m. system between the direction of scattering and the initial direction of motion of either particle.

<sup>c</sup> Corrected for accidental and blank counts.

<sup>d</sup> The analyzing efficiency is defined as (five-fold rate)/(ABC rate).

Table IV. Experimentally measured asymmetries of the analyzed recoil protons<sup>a</sup>

Mean c. m. scattering angle (deg)	Run 1 <sup>b</sup>		Run 2 <sup>c</sup>	
	Left <sup>d</sup>	Right <sup>d</sup>	Left	Right
114.2	-0.132±0.089	-0.074±0.066	+0.005±0.039	+0.039±0.033
124.5	—————	—————	+0.099±0.054	-0.091±0.038
133.8	+0.130±0.064	-0.212±0.053	+0.068±0.031	-0.039±0.031
145.2	+0.045±0.053	-0.073±0.038	+0.046±0.031	-0.123±0.028

<sup>a</sup>The errors given are standard deviations and are due to counting statistics only.

<sup>b</sup>All Run-1 asymmetries are based on the results of the film analysis, except the 133.8-deg (left) asymmetry, for which only electronic data exist.

<sup>c</sup>The asymmetries measured with each analyzing telescope were combined in order to obtain the Run-2 asymmetries given here. A total of 800 to 2000 analyzed recoil protons determined each Run-2 asymmetry listed.

<sup>d</sup>The "Left" and "Right" column headings refer to the side of the incident pion beam on which the recoil protons were observed.

Table V. Summary of experimental results

Experimental quantity	Run No.	Mean c. m. scattering angle (deg)			
		114.2	124.5	133.8	145.2
Recoil-proton asymmetry ( $\bar{e}$ ) <sup>a</sup>	1	+0.002±0.055	————	-0.178±0.043	-0.063±0.034
	2	+0.020±0.027	-0.094±0.032	-0.054±0.023	-0.088±0.022
Analyzing ability ( $\bar{F}_2$ ) <sup>b</sup>	1	+0.276±0.047	————	+0.407±0.043	+0.452±0.041
	2	+0.413±0.048	+0.573±0.046	+0.500±0.047	+0.517±0.023
Recoil-proton polarization ( $\bar{P}_1 = \bar{e}/\bar{F}_2$ )	1	+0.007±0.199	————	-0.438±0.116	-0.139±0.076
	2	+0.048±0.065	-0.164±0.057	-0.108±0.047	-0.170±0.043
Recoil-proton polarization <sup>c</sup>	1 and 2	+0.044±0.062	-0.164±0.057	-0.155±0.044	-0.162±0.037

<sup>a</sup>These results were obtained by combining the Left and Right asymmetries of Table IV at each scattering angle, after reversing the sign of the Left asymmetry and after adding (in rms fashion) to each statistical counting error in Table IV the beam-center-line uncertainty discussed in Section VI-A.

<sup>b</sup>We determined each analyzing ability by computing  $\bar{P}_2 = \bar{P}_2^{(C)} = \bar{e}^{(C)} / \bar{P}_1^{(C)}$ , where  $\bar{e}^{(C)}$  is the appropriate asymmetry that was measured during the calibration portion of the experiment, and  $\bar{P}_1^{(C)}$  is the polarization of the proton beam used in the calibration measurement. The errors presented here arise from the experimental uncertainties in the calibration asymmetries (counting statistics and beam-center-line uncertainty). The error in  $\bar{P}_1^{(C)}$  is not included. The results of both analyzing telescopes in Run 2 have been combined.

<sup>c</sup>These final polarization values were obtained by combining the results of Runs 1 and 2. A plot of these values is given in Fig. 1 of Foote et al.<sup>16</sup> The errors are assumed to be independent.

LEGENDS

Fig. 1. Scale drawing of the magnet system for the  $\pi^+$  beam. The bending magnets are designated  $M_1$  and  $M_2$ ;  $Q_1$ ,  $Q_2$ , and  $Q_3$  are the quadrupole focusing magnets. Magnets  $Q_1$  and  $Q_3$  have 8-in. apertures, and  $Q_2$  has a 4-in. aperture. Also shown is the counter arrangement used to detect the recoil-proton polarization. The dimensions of the counters and carbon target are not to scale.

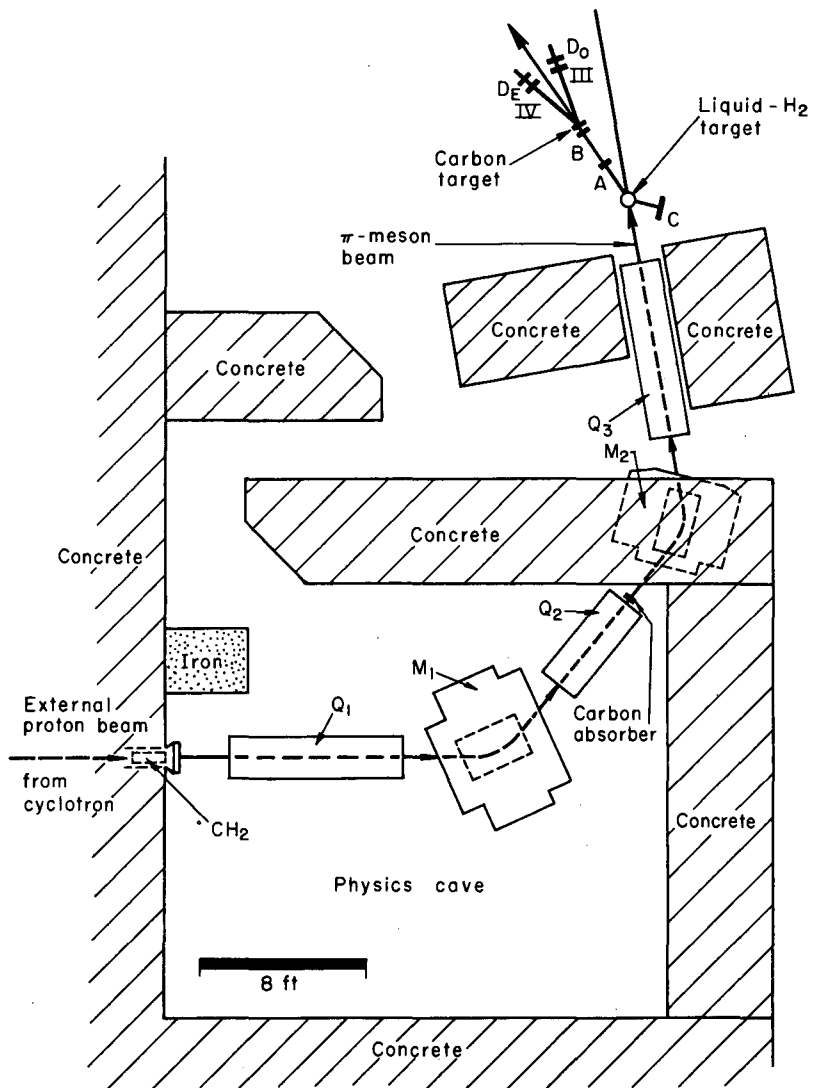
Fig. 2. Scale drawing (plan view) of counter and target arrangement used to measure the polarization of the recoil protons.

Fig. 3. Scale drawing (elevation view) of counters, targets, and principal supporting frameworks used to measure the polarization of the recoil protons. The angles  $\Theta_1$  and  $\Theta_2$  have been set equal to 0 deg in this figure. Only one analyzing telescope is shown.

Fig. 4. Range curve of the recoil-proton beam at  $\Theta_1 = 16.9$  deg right.

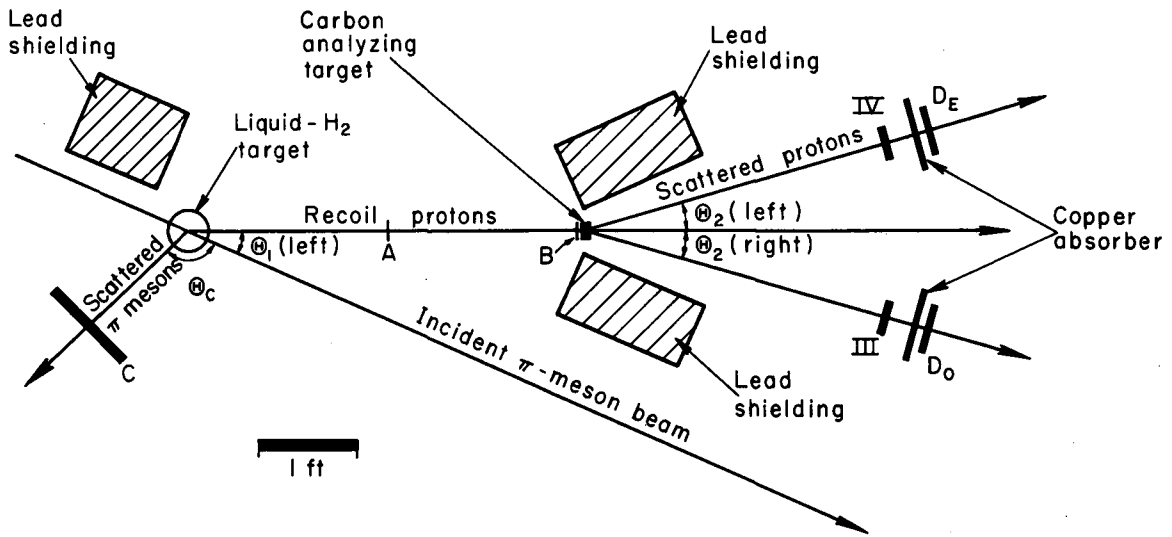
Fig. 5. Beam profile of the recoil-proton beam at  $\Theta_1 = 16.9$  deg left.

The angular reading of the profile center line lies near 8 deg rather than 0 deg because the point from which the plumb bob hung was not at the center of the counter telescope.



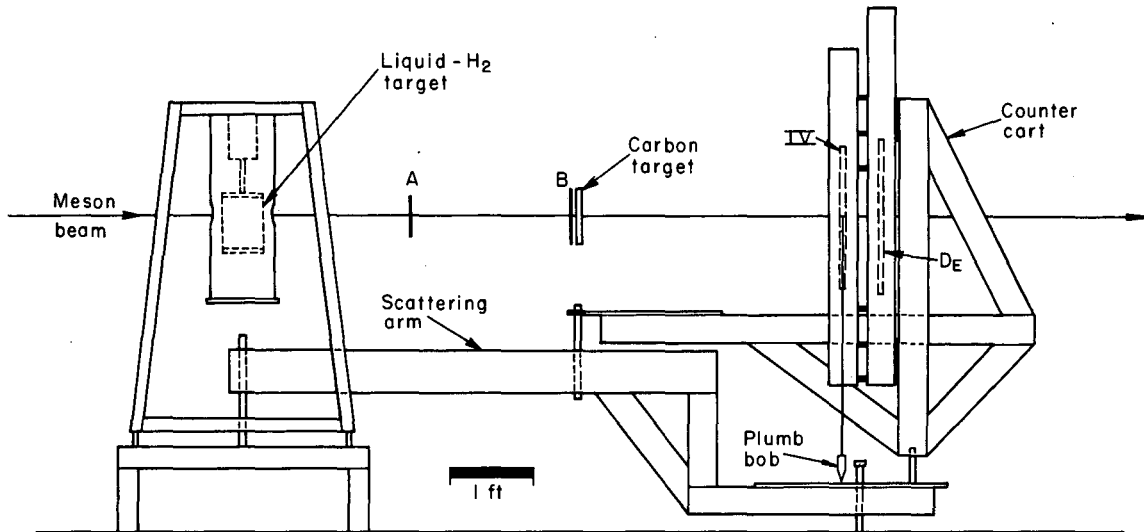
MU-20227

Fig. 1.



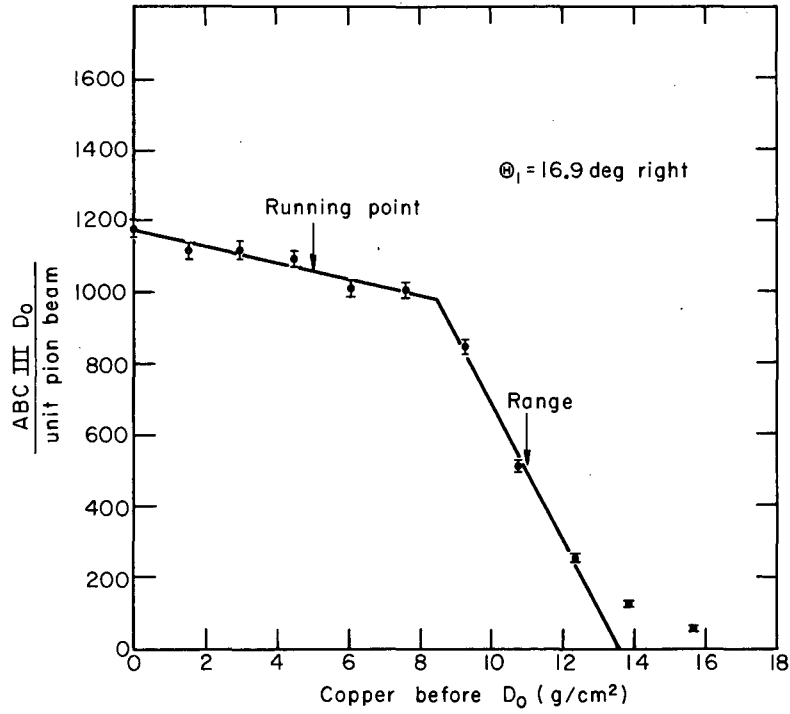
MU-20228

Fig. 2.



MU-2029

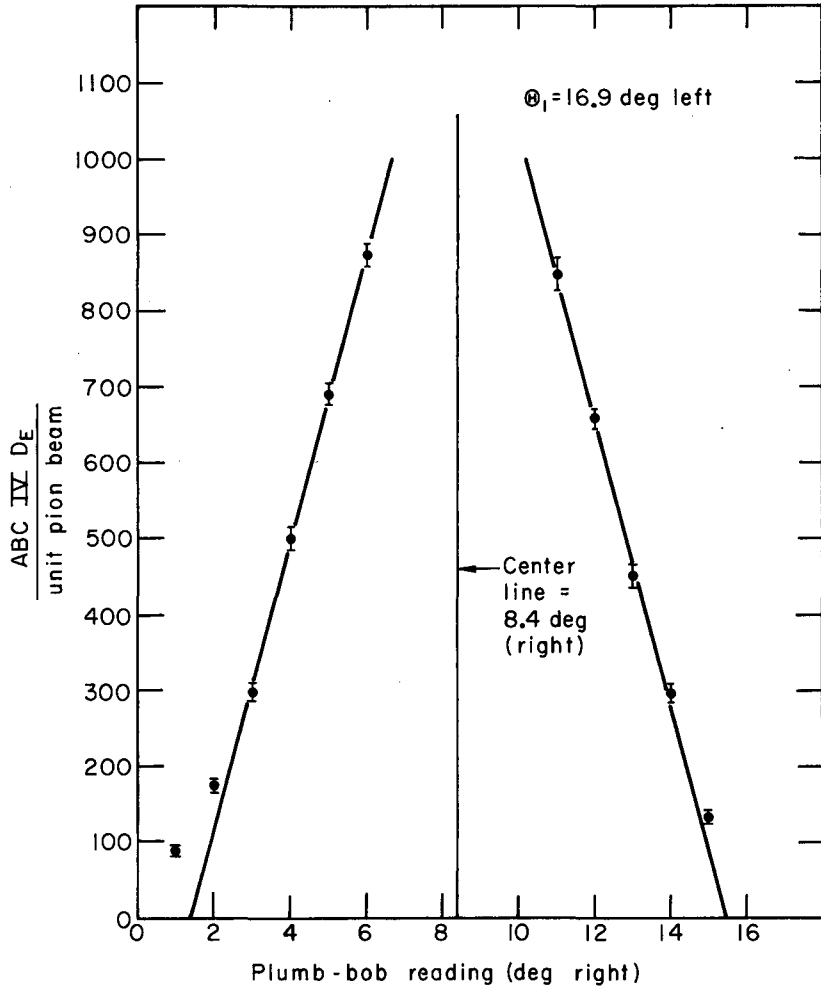
Fig. 3.



MU-20230

Fig. 4.





MU-20231

Fig. 5.

This report was prepared as an account of Government sponsored work. Neither the United States, nor the Commission, nor any person acting on behalf of the Commission:

- A. Makes any warranty or representation, expressed or implied, with respect to the accuracy, completeness, or usefulness of the information contained in this report, or that the use of any information, apparatus, method, or process disclosed in this report may not infringe privately owned rights; or
- B. Assumes any liabilities with respect to the use of, or for damages resulting from the use of any information, apparatus, method, or process disclosed in this report.

As used in the above, "person acting on behalf of the Commission" includes any employee or contractor of the Commission, or employee of such contractor, to the extent that such employee or contractor of the Commission, or employee of such contractor prepares, disseminates, or provides access to, any information pursuant to his employment or contract with the Commission, or his employment with such contractor.